# Multimodal method for flow-induced acoustic resonance in successive deep axisymmetric cavities in a duct

Xiwen Dai and Yves Aurégan
Laboratoire d'Acoustique de l'Université du Maine, Avenue Olivier Messiaen 72085, Le Mans, Cedex 9, France

**Summary**
Flow-induced pulsations in axisymmetric cavities with an incident sound wave are investigated. The underlying physics of the problem, which is the interaction between the shear layer instabilities and acoustic waves, is study by means of multimodal analysis. The configuration is considered as a series of duct segments with different radius. For a sheared mean flow, the radial modes of different duct segments are solved. Matching the modes at the interfaces between the segments gives the acoustic scattering matrix and the acoustic fields of the cavities-duct system for plan wave incidence. It is found that the sound amplification rate is determined by the intensity of the unstable hydrodynamic mode. Multi-cavity system tends to give more significant sound amplification than a single cavity.

**PACS no. 43.28.Ra, 43.20.Mv**

## 1. Introduction

There may be a strong interaction between flow and acoustic when a free shear layer is formed. This is the case for instance in the T-junctions, in corrugated pipes [1], … On the other hand, it has been demonstrated that instabilities can also occur in lined ducts treat by locally reacting liners [2] or by porous materials [3]. The purpose of this work is to go from discrete systems, e.g. corrugated tubes, to continuous systems where the wall behavior is described by continuous impedance. This paper is a first step in this direction. It validates the used tools i.e. a multimodal method in shear flow.

The acoustical behavior of axisymmetric cavities in a flow duct is studied. Between the cavity and the duct a shear layer is formed. In most cases this shear layer is unstable. Hydrodynamic perturbations created at the upstream edge of the cavity are convected by the flow while being amplified. When the amplification rate is sufficiently high, the shear layer is rolled into discrete vortices. This nonlinear saturation mechanism is not considered in this work that is concentrated on the linear behavior of the system. Thus only the energy exchanges between the flow and the acoustic are of interest and the flow-induced pulsations that result from a coupling of a linear amplification with a resonance are not considered here. The energy that a flow can give to the acoustic is maximum when the Strouhal number based of the sound frequency, the length of the cavity and the convection velocity $U_\Gamma$ of the unstable hydrodynamic mode is of the order of 1: $S_\Gamma = fL_c/U_\Gamma \sim 1$ . The flow can also provide energy to the acoustic when the length of the cavity is an entire number of hydrodynamic wavelengths i.e. $S_\Gamma \sim 1, 2, 3 \cdots$.When this condition of entire Strouhal number is verified near a resonance frequency of the cavity a very high amplification is obtained [4]. Those high amplifications can be unrealistic in our modeling because of the nonlinear phenomena that can occur in this case.

The numerical model used in this paper is the MultiModal Method solving the Linearized Euler Equations [5]. The shear flow modes (acoustic and hydrodynamic) are computed in the duct and in the cavity segments. Matching the modes at the interfaces between the segments gives the acoustic scattering matrix and the acoustic fields of the cavities-duct system for any incident wave. This shows the coupling of the shear layer and the acoustic waves.

## 2. Multimodal method

The axisymmetric cavities-duct is sketched in figure 1(a). Such configuration can be considered as a series of identical cells, as shown in figure 1(b), each of which is split into three segments: duct 1-3 with radius $R_1$, $R_2$, and $R_1$ respectively. A parallel non-uniform mean flow is present in the ducts. The mean flow profile is assumed to be unaltered at the interfaces between adjacent segments. Thus, the mean flow profile is the same everywhere when the radius is smaller than $R_1$ and the mean flow is supposed to be 0 in the cavity.

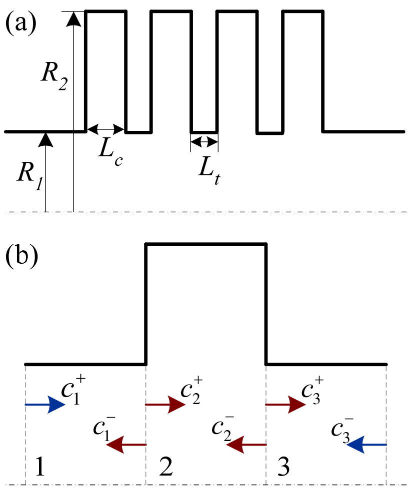


Figure 1. (a) Successive axisymmetric cavities in a duct, (b) duct-cavity-duct cell.

### 2.1. Finding the modes

Linearization of the Euler equations for conservation of momentum and mass gives:

$$\rho_0\left(\frac{\partial}{\partial t}+U\frac{\partial}{\partial z}\right)u'+\rho_0\frac{\mathrm{d}U}{\mathrm{d}r}v'=-\frac{\partial p'}{\partial z}, \tag{1}$$

$$\rho_0\left(\frac{\partial}{\partial t}+U\frac{\partial}{\partial z}\right)v'=-\frac{\partial p'}{\partial r}, \tag{2}$$

$$\frac{1}{\rho_0 c_0^2}\left(\frac{\partial}{\partial t}+U\frac{\partial}{\partial z}\right)p'=-\left(\frac{\partial u'}{\partial z}+\frac{\partial v'}{\partial r}+\frac{v'}{r}\right), \tag{3}$$

where $\rho_0$ is the mean density, $c_0$ is speed of sound, and $U$ is the mean flow velocity. $u'$ and $v'$ are the linear velocity disturbance in respectively the z- and r-direction, and $p'$ is the linear pressure disturbance. Applying $\rho_0\left(\partial/\partial t+U\,\partial/\partial z\right)$ to (3) and subtracting $\partial p'/\partial z$ (1) and $\partial p'/\partial r$ (2) gives:

$$\frac{1}{c_0^2}\left(\frac{\partial}{\partial t}+U\frac{\partial}{\partial z}\right)^2 p'-\left(\frac{\partial^2 p'}{\partial z^2}+\frac{\partial^2 p'}{\partial r^2}+\frac{1}{r}\frac{\partial p'}{\partial r}\right) =2\rho_0\frac{\mathrm{d}U}{\mathrm{d}r}\frac{\partial v'}{\partial z} \tag{4}$$

The quantities are put in dimensionless form by:

$$p_*=\frac{1}{\rho_0 c_0^2}p',\ (z_*,r_*)=(\frac{z}{R_1},\frac{r}{R_1}),$$
$$(u_*,v_*)=\frac{1}{c_0}(u',v'),\ \omega_*=\frac{\omega R_1}{c_0}, \tag{5}$$
$$M(r)=M_0 f(r)=\frac{1}{c_0}U(r),\ t_*=\frac{c_0 t}{R_1},$$

where $\omega$ is the frequency, and M is the Mach number. The function $f(r)$ prescripts the mean flow profile. $M_0$ is the average Mach number in the duct. The dimensionless form of equations (2) and (5) is:

$$\left(\frac{\partial}{\partial t_*}+M_0 f\frac{\partial}{\partial z_*}\right)v_*=-\frac{\partial p_*}{\partial r_*}, \tag{6}$$

$$\left(\frac{\partial}{\partial t_*}+M_0 f\frac{\partial}{\partial z_*}\right)^2 p_* -\left(\frac{\partial^2}{\partial z_*^2}+\frac{\partial^2}{\partial r_*^2}+\frac{1}{r_*}\frac{\partial}{\partial r_*}\right)p_*=2M_0\frac{\mathrm{d}f}{\mathrm{d}r_*}\frac{\partial v_*}{\partial z_*}. \tag{7}$$

With the following assumption of harmonic waves in the z-direction:

$$p_*=P(r_*)\exp(-ik_*z_*)\exp(i\omega_*t_*),$$
$$v_*=V(r_*)\exp(-ik_*z_*)\exp(i\omega_*t_*), \tag{8}$$
$$q_*=Q(r_*)\exp(-ik_*z_*)\exp(i\omega_*t_*),$$

where $\mathrm{i}^2=-1$, $q_*=\mathrm{i}\,\partial p_*/\partial z_*$ and $k_*$ is the dimensionless wavenumber, equations (6) and (7) gives:

$$i(\omega_*-M_0 f k_*)V=-\frac{\mathrm{d}P}{\mathrm{d}r_*}, \tag{9}$$

$$\left(1-M_0^2f^2\right)k_*^2P+2\omega_*M_0 f k_*P-\omega_*^2P -\frac{\mathrm{d}^2P}{\mathrm{d}r_*^2}-\frac{1}{r_*}\frac{\mathrm{d}P}{\mathrm{d}r_*}=-2iM_0\frac{\mathrm{d}f}{\mathrm{d}r_*}k_*V. \tag{10}$$

The equations (9) and (10) are discretized in the $r$-direction by taking $N_1$ equally spaced points in duct 1and 3, and $N_2$ equally spaced points in duct 2. The spacing between interior points in all ducts is $\Delta r=R_1/N_1=R_2/N_2$, and the first and last points are taken $\Delta r/2$ from the axial line and the duct wall. The finite difference method is used to solve the problem. The following generalized eigenvalue problem is found:

$$k_*\begin{pmatrix}\mathbf{I}-M_0^2\mathbf{f}^2 & 2iM_0\mathbf{f_a} & \mathbf{0}\\ \mathbf{0} & iM_0\mathbf{f} & \mathbf{0}\\ \mathbf{0} & \mathbf{0} & \mathbf{I}\end{pmatrix}\begin{pmatrix}\mathbf{Q}\\ \mathbf{V}\\ \mathbf{P}\end{pmatrix}= \begin{pmatrix}-2\omega_*M_0\mathbf{f} & \mathbf{0} & \omega_*^2\mathbf{I}+\mathbf{D_2}+\mathbf{r}_*^{-1}\mathbf{D_1}\\ \mathbf{0} & i\omega_*\mathbf{I} & \mathbf{D_1}\\ \mathbf{I} & \mathbf{0} & \mathbf{0}\end{pmatrix}\begin{pmatrix}\mathbf{Q}\\ \mathbf{V}\\ \mathbf{P}\end{pmatrix}, \tag{11}$$

$\mathbf{I}$ is the identity matrix, $\mathbf{f}$, $\mathbf{f_2}$ and $\mathbf{f_a}$ are diagonal matrices with on the diagonal the values of $f$, $f^2$ and $df/dr_*$ at the discrete points in the ducts. The $\mathbf{D_1}$ and $\mathbf{D_2}$ are matrices for the first and second order differential operator with respect to $r_*$. The boundary condition $dp_*/dr_* = 0$ on the axial line and the duct wall are taken into account in the differential operator matrices. Matrix $\mathbf{r}_*^{-1}\mathbf{D_1}$ represents the discretization of $(1/r_*)dP/dr_*$. Solving the above eigenvalue problem gives the modes and the corresponding wavenumbers in the ducts. In duct 1 and 3, $3N_1$ modes are found, including $N_1$ acoustic modes propagating or decaying in the +$z$ direction, $N_1$ acoustic modes propagating or decaying in the -$z$ direction, and $N_1$ hydrodynamic modes propagating in the +$z$ direction. In duct 2, there are $N_2$ acoustic modes propagating or decaying both in the +$z$ direction and in the –$z$ direction. However, since the sheared mean flow is only present in the first $N_1$ discrete point, a number of $N_1$ of hydrodynamic modes are found. In each duct, the total solution for $p_*$, $v_*$, and $q_*$ is a linear combination of the solved modes:

$$\begin{aligned}
\mathbf{q}_*(z_*,t_*) &= \sum_{n=1}^{N} \mathbf{C}_n \mathbf{Q}_{e,n} \exp\left(-ik_{e,n*}z_*\right)\exp\left(i\omega_* t_*\right),\\
\mathbf{v}_*(z_*,t_*) &= \sum_{n=1}^{N} \mathbf{C}_n \mathbf{V}_{e,n} \exp\left(-ik_{e,n*}z_*\right)\exp\left(i\omega_* t_*\right),\\
\mathbf{p}_*(z_*,t_*) &= \sum_{n=1}^{N} \mathbf{C}_n \mathbf{P}_{e,n} \exp\left(-ik_{e,n*}z_*\right)\exp\left(i\omega_* t_*\right).
\end{aligned} \tag{12}$$

## 2.2. Mode matching

Once the modes are solved in each duct segment, they are linked by continuity conditions at the interfaces between the adjacent segments and by a rigid wall condition had to be applied at $z_* = 0$ and $z_* = l_c$ for $1 > r_* > r_2$. For the discrete points, $0 < r_* < 1$, the continuity of $p_*$, $v_*$, and $q_*$ can be deduced from the linearized conservations of mass, momentum and energy. For the points on the vertical walls in duct 2, the axial velocity vanishes and so $q_* = 0$. These conditions give:

$$\underbrace{\begin{pmatrix}
\mathbf{0} & -\mathbf{Q}_1^- & \mathbf{Q}_2^+ & \mathbf{Q}_2^-\mathbf{E}_C^- \\
\mathbf{0} & \mathbf{0} & & \\
\mathbf{0} & -\mathbf{V}_1^- & \mathbf{V}_2^+ & \mathbf{V}_2^-\mathbf{E}_C^- \\
\mathbf{0} & -\mathbf{P}_1^- & \mathbf{P}_2^+ & \mathbf{P}_2^-\mathbf{E}_C^- \\
-\mathbf{Q}_1^+ & \mathbf{0} & \mathbf{Q}_2^+\mathbf{E}_C^+ & \mathbf{Q}_2^- \\
\mathbf{0} & \mathbf{0} & & \\
-\mathbf{V}_1^+ & \mathbf{0} & \mathbf{V}_2^+\mathbf{E}_C^+ & \mathbf{V}_2^- \\
-\mathbf{P}_1^+ & \mathbf{0} & \mathbf{P}_2^+\mathbf{E}_C^+ & \mathbf{P}_2^-
\end{pmatrix}}_{\mathbf{S_A}}
\begin{pmatrix}\mathbf{C}_3^+\\ \mathbf{C}_1^-\\ \mathbf{C}_2^+\\ \mathbf{C}_2^-\end{pmatrix}
=
\underbrace{\begin{pmatrix}
\mathbf{Q}_1^+\mathbf{E}_D^+ & \mathbf{0}\\
\mathbf{0} & \mathbf{0}\\
\mathbf{V}_1^+\mathbf{E}_D^+ & \mathbf{0}\\
\mathbf{P}_1^+\mathbf{E}_D^+ & \mathbf{0}\\
\mathbf{0} & \mathbf{Q}_1^-\mathbf{E}_D^-\\
\mathbf{0} & \mathbf{0}\\
\mathbf{0} & \mathbf{V}_1^-\mathbf{E}_D^-\\
\mathbf{0} & \mathbf{P}_1^-\mathbf{E}_D^-
\end{pmatrix}}_{\mathbf{S_B}}
\begin{pmatrix}\mathbf{C}_1^+\\ \mathbf{C}_3^-\end{pmatrix} \tag{13}$$

Equation (13) gives the scattering matrix: $\mathbf{S} = \mathbf{S}_A^{-1}\mathbf{S}_B$, which relates all the waves propagating away from the cavity in the duct to the waves propagating towards the cavity:

$$\begin{pmatrix}\mathbf{C}_3^+\\ \mathbf{C}_1^-\\ \mathbf{C}_2^+\\ \mathbf{C}_2^-\end{pmatrix} = \mathbf{S}\begin{pmatrix}\mathbf{C}_1^+\\ \mathbf{C}_3^-\end{pmatrix}. \tag{14}$$

For plane wave, the transmission and reflection coefficients of the cavity can be defined in either direction,

$$\begin{aligned}
T^+ &= \mathbf{C}_3^+(1)/\mathbf{C}_1^+(1) = \mathbf{S}(1,1),\\
R^+ &= \mathbf{C}_1^-(1)/\mathbf{C}_1^+(1) = \mathbf{S}(2N_1+1,1),\\
T^- &= \mathbf{C}_1^-(1)/\mathbf{C}_3^-(1) = \mathbf{S}(2N_1+1,2N_1+1),\\
R^- &= \mathbf{C}_3^+(1)/\mathbf{C}_3^-(1) = \mathbf{S}(1,2N_1+1).
\end{aligned} \tag{15}$$

# 3. Results

## 3.1. Interaction between hydrodynamic instabilities and acoustic waves

A hyperbolic-tangent profile is used,

$$\begin{aligned}
f_0(r_*) &= 1 - \left(1 + m\exp\left(m\phi(m)\frac{r_{\inf} - r_*}{\theta}\right)\right)^{-\frac{1}{m}},\\
\phi(m) &= \int_0^1 \frac{1-z}{1-z^m}dz,
\end{aligned} \tag{16}$$

where $m$ is the profile parameter, $\theta$ is the momentum thickness of the shear layer, the inflexion point is set at $r_{\inf}$. To ensure that the mean flow velocity is zero at the wall of duct 1, and the section-averaged value of the profile function equals unity, the following treatment of the profile function is needed,

$$f(r_*) = \begin{cases} \dfrac{f_0(r_*) - f_0(r_1)}{2\int_0^{r_1}\left[f_0(r_*) - f_0(r_1)\right]r_* dr_*}, & 0 \le r_* \le r_1,\\ 0, & r_1 < r_* \le r_2. \end{cases} \tag{17}$$

In this subsection, the profile parameters are set as: m=1, $r_{\inf}$=1, $\theta$=0.1.

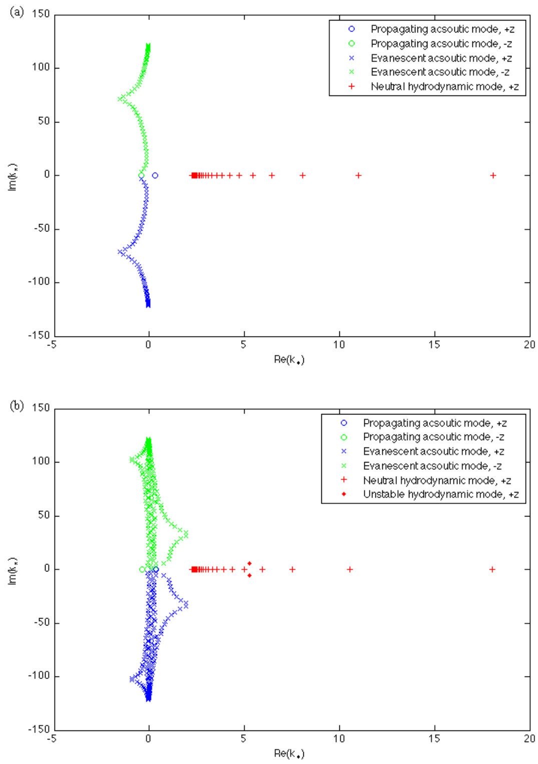


Figure 2. Non-dimensional wave numbers of the modes in: a) duct 1 and 3, b) duct 2(cavity segment).

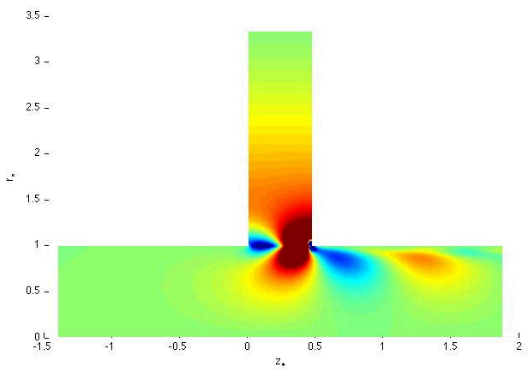


Figure 3. Linear velocity disturbance $v_{r*}$ field.

Figure 2 shows the dimensionless wave numbers of the modes in duct 1 (and 3) and duct 2 (cavity segment) for $R_1$=15mm, $R_2$=50mm, $L_C$=7mm, $L_T$=0.5mm, $M_0$=0.1, $f$=1000 Hz, and $N_1$=90. In duct 1 the propagating and evanescent acoustic modes in the $+z$ and $-z$ directions, the neutral hydrodynamic modes propagating in the $+z$ direction are found. In the cavity segment, two hydrodynamic modes are found with non-zero imaginary part such that the mode grows and decays exponentially in the propagation direction. The one with positive imaginary part is the unstable hydrodynamic mode corresponding to the "Kelvin-Helmholtz" type instability of the shear layer. The radial velocity $v_{r*}$ is shown in figure 3, the unstable hydrodynamic wave in the shear layer can be seen.

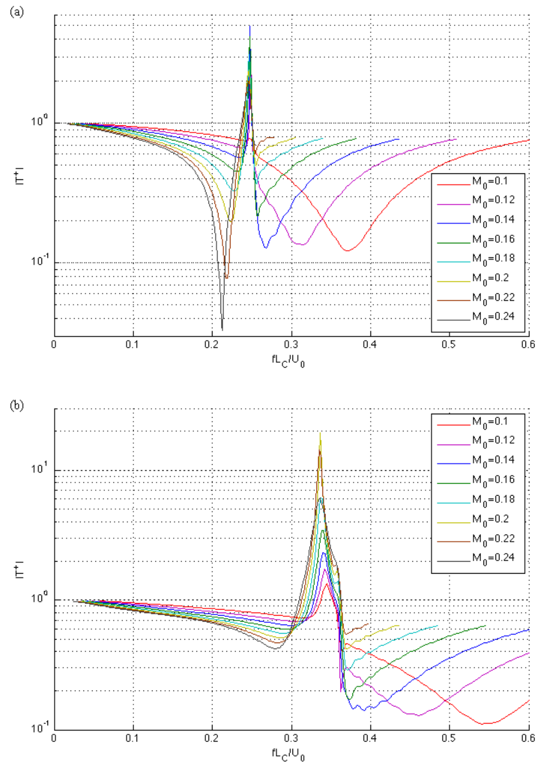


Figure 4. Magnitude of transmission coefficient of one cavity as a function of Strouhal number, (a) $R_1$=15mm, $R_2$=50mm, $L_C$=7mm, (b) $R_1$=15mm, $R_2$=50mm, $L_C$=10mm.

In figure 4, the magnitudes of $T^+$ for plane wave are plot against the Strouhal number based on the mean velocity $S_t = fL_c/U_0$ for different Mach number. It is found that the peak frequencies of amplification for each$M_0$ happen at nearly the same Strouhal number. However, the Strouhal number for the peak amplification varies as the length of the cavity is increased. The corresponding imagery parts of the wavenumbers are shown in figure 5. Im($k_{hu*}$) is the growth rate of the disturbance. We can find that the growth rates for the peaks in figure 4, as marked in figure 5, are not the maximum.

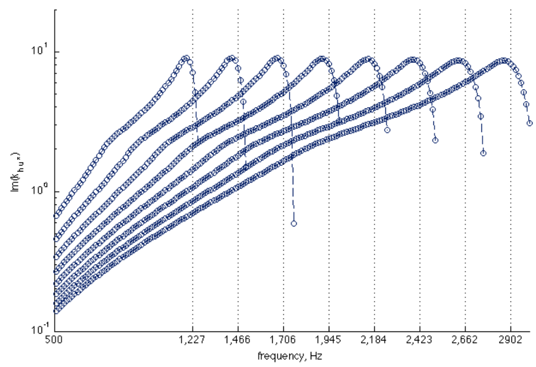


Figure 5. Imaginary part of the wave number of the unstable hydrodynamic mode of the shear layer.

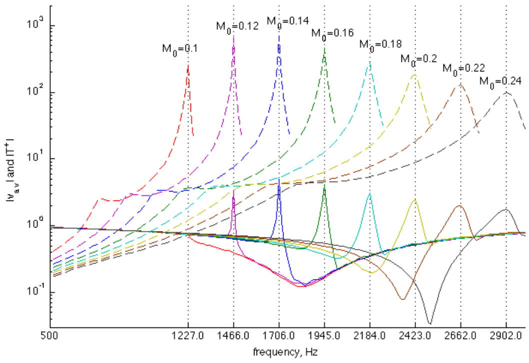

Figure 6. Magnitude of transmission coefficient (solid lines) and magnitude of the fluctuating average velocity at the cavity opening caused by the unstable hydrodynamic mode (dashed lines).

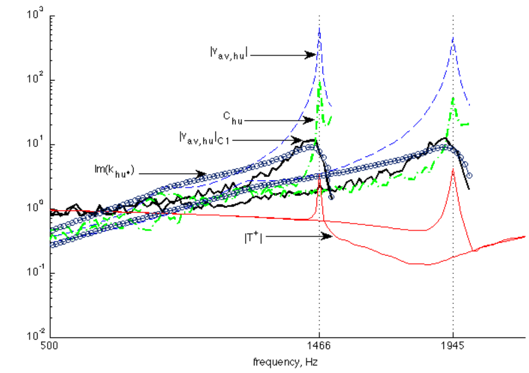

Figure 7. Magnitude of the fluctuating average velocity at the cavity opening caused by the unstable hydrodynamic mode $|v_{av,hu}|$, $|C_{hu}|$, $|v_{av,hu}|$ for $|C_{hu}|=1$ (denoted as $|v_{av,hu}|_{C1}$), growth rate $Im(k_{hu})$, and magnitude of transmission coefficient $|T^+|$ as a function of incident frequency.

In figure 6, the magnitude of $T^+$, accompanied with the magnitude of the fluctuating average velocity (along the length of the cavity opening) due to the unstable hydrodynamic mode, are plot against frequency. It is shown that the peak frequencies for $T^+$ and $|v_{av,hu}|$ coincide. It indicates that the peak sound amplification occurs when the magnitude of the fluctuating flow flux through the cavity opening caused by the shear layer instabilities reaches its maximum.

We insolated the velocity disturbance due to unstable hydrodynamic mode from equation (12),

$$\mathbf{v}_{hu*}(z_*,t_*)=C_{hu}\mathbf{V}_{hu}\exp(-ik_{hu*}z_*)\exp(i\omega_* t_*). \quad (18)$$

The effects determining $|v_{av,hu}|$ can be classified into: $\mathbf{V}_{hu}\exp(-ik_{hu*}z_*)$, which is related to the growth rate and convection velocity of the vortical disturbance; $C_{hu}$, which is the result of the coupling of the hydrodynamic modes and the acoustic waves. In figure 7, $|v_{av,hu}|$ for $|C_{hu}|=1$ (denoted as $|v_{av,hu}|_{C1}$), $|C_{hu}|$, and $Im(k_{hu})$ are also plot. It is found that the peak amplification frequencies are not the frequencies at which the shear layer is most unstable, but in the neighborhood of it. On the other hand, peak amplification frequencies are found exactly the peak value frequencies of $|C_{hu}|$. So, it can be deduced that the flow-induced sound amplification originates from the inherent instabilities of the shear layer, but defining the peak amplification involves the shear layer properties, the incident sound wave, and the cavity. In practice, the peak amplification frequency and the amplification ratio are also influenced by the nonlinear effects in the flow that are beyond the present investigation.

### 3.2. Successive axisymmetric cavities

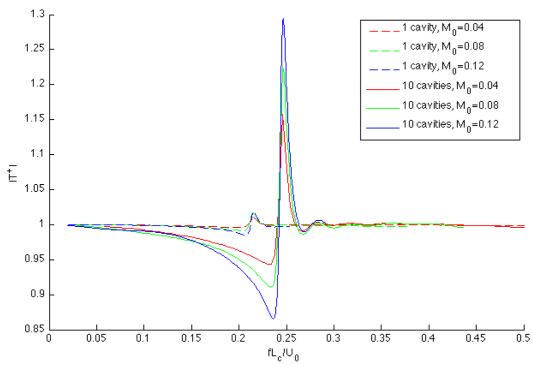


Figure 8. Magnitude of transmission coefficient as a function of Strouhal number for 1 cavity (dashed lines) and 10 successive cavities (solid lines).

For one cavity equation (14) gives,

$$\begin{pmatrix}\mathbf{C}_1^-\\ \mathbf{C}_3^+\end{pmatrix}=\mathbf{S}^{(1)}\begin{pmatrix}\mathbf{C}_1^+\\ \mathbf{C}_3^-\end{pmatrix} \quad (19)$$

then the scattering matrix for two cavities can be given by the following relations:

$$\mathbf{S}^{(1+2)}=\begin{bmatrix}\mathbf{S}_{11}^{(2)}\mathbf{E}\mathbf{S}_{11}^{(1)} & \mathbf{S}_{12}^{(2)}+\mathbf{S}_{11}^{(2)}\mathbf{S}_{12}^{(1)}\mathbf{F}\mathbf{S}_{22}^{(2)}\\ \mathbf{S}_{21}^{(1)}+\mathbf{S}_{22}^{(1)}\mathbf{S}_{21}^{(2)}\mathbf{E}\mathbf{S}_{11}^{(1)} & \mathbf{S}_{22}^{(1)}\mathbf{F}\mathbf{S}_{22}^{(2)}\end{bmatrix} \quad (20)$$

$$\mathbf{E}=\left(\mathbf{I}-\mathbf{S}_{12}^{(1)}\mathbf{S}_{21}^{(2)}\right)^{-1},\quad \mathbf{F}=\left(\mathbf{I}-\mathbf{S}_{21}^{(2)}\mathbf{S}_{12}^{(1)}\right)^{-1}$$

The above iterative scattering matrix algorithm [6] is employed to obtain the scattering matrix of a series of the cavities. The magnitude of the transmission coefficient for1 cavity and 10 cavities are shown in figure 8. The geometrical parameters are$R_1$=15mm, $R_2$=19mm, $L_C$=4mm, $L_T$=8mm. The mean flow profile is given by equations (16) and (17)for m=1, $r_{inf}$ =1, $\theta$=0.05.It is found that the cavities shows both sound absorption and sound amplification properties as the Strouhal number increases. The peak amplification occurs at the same Strouhal number. Due to the accumulative effect, the 10-

cavityconfiguration has higher peaks than one cavity.

## 4. Conclusions

A theoretical linear model based on the multimodal method is established to study the sound amplification problem caused by the vortical-acoustic wave interaction. The present model is able to take the boundary layer effects into account. It is found that due to the interaction between the incident sound wave, the shear layer, and the cavity, an intense unstable hydrodynamic mode can be produced, and the incident sound wave is significantly amplified. Due to the accumulative effects, multi-cavity system tends to give more significant sound amplification than a single cavity.

### Acknowledgement

This work has been funded by Le Mans Acoustique project and the ITN project FlowAirS (European Grant No. FP7-PEOPLE-2011-ITN-289352).

### References

[1]D. Tonon, A. Hirschberg, J. Golliard, and S. Ziada: Aeroacoustics of pipe systems with closed branches. Int. J. Aeroacoust.10(2011)201–276.

[2]D. Marx, Y. Aurégan, H Bailliet and J.C. Valière: PIV and LDV evidence of hydrodynamic instability over a liner in a duct with flow. J. Sound Vib. 329(2010) 3798–3812.

[3]Y. Aurégan and D. K. Singh: Experimental observation of a hydrodynamic mode in a flow duct with a porous material. J. Acoust. Soc. Am. 136(2014) 567–572

[4]S.W. Rienstra, A. Hirschberg: An Introduction to Acoustics, Eindhoven University of Technology (2012)

[5] G. Kooijman, P. Testud, Y. Aurégan, A. Hirschberg: Multimodal method for scattering of sound at a sudden expansion in a duct with subsonic flow. J. Sound Vib. 310(2008) 902–922.

[6] G.D. Furnell and D.A. Bies: Matrix analysis of acoustic wave propagation within curved ducting systems. J. Sound Vib. 132(1989) 245–263.